REPORT DOCUMENTATION PAGE

AFRL-SR-AR-TR-02-

0328

1. AGENCY USE ONLY *(Leave blank)*

2. REPORT DATE

3. REPORT TYPE AND DATES COVERED
5/1/99 TO 4/30/02 Final

4. TITLE AND SUBTITLE
Crossed-Field, High Energy Microwave Source Experiments and Theory

5. FUNDING NUMBERS
61102f
2301/EX

6. AUTHOR(S)
Prof. Gilgenbach

7. PERFORMING ORGANIZATION NAME(S) AND ADDRESS(ES)
University of Michigan
1058 Wolverine Tower-DRDA
3003 S State Street
Ann Arbor, MI 48109-1274

8. PERFORMING ORGANIZATION REPORT NUMBER

9. SPONSORING/MONITORING AGENCY NAME(S) AND ADDRESS(ES)
Department of the Air Force
Air Force Office of Sdentific Research
801 N. Randolph St Rm 732
Arlington. VA 22203-1977

10. SPONSORING/MONITORING AGENCY REPORT NUMBER
F49620-99-1-0255

11. SUPPLEMENTARY NOTES

12a. DISTRIBUTION AVAILABILITY STATEMENT
Distribution Statement A. Approved for public release; distribution is unlimited.

12b. DISTRIBUTION CODE

13. ABSTRACT *(Maximum 200 words)*
Relativistic magnetron experiments have successfully been accomplished utilizing the MELBA accelerator at parameters of -300 to -400 kV, 1-10 kA and pulselengths of -0.5 microseconds. A major accomplishment has been the installation of a ceramic insulator stack, which has improved the base vacuum by a factor of 10 from 10-0 Torr scale to the 10-i Torr scale. The Titan-Pulse Sciences magnetron is a 6-vane device operating at about 1 GHz. Microwave power has been extracted from two-opposing-cavities of this magnetron. Assuming equal output power in both arms, peak, extracted microwave power between 120 MW and 400 MW has been achieved. Microwave pulse shortening is observed with typical pulselengths in the range between 10 ns and 100 ns. Time-frequency analysis has been utilized for mode identification, indicating both the pi-mode and the 213 -pi mode.

14. SUBJECT TERMS

15. NUMBER OF PAGES

16. PRICE CODE

17. SECURITY CLASSIFICATION OF REPORT	18. SECURITY CLASSIFICATION OF THIS PAGE	19. SECURITY CLASSIFICATION OF ABSTRACT	20. LIMITATION OF ABSTRACT
Unclassified	Unclassified	Unclassified	UL

FINAL TECHNICAL REPORT TO:

Dr. ROBERT J. BARKER
THE AIR FORCE OFFICE OF SCIENTIFIC RESEARCH

FOR THE PROJECT:

CROSSED FIELD, HIGH ENERGY MICROWAVE SOURCE EXPERIMENTS AND THEORY

AFOSR GRANT NUMBER: F49620-99-1-0255

SUBMITTED BY:

RONALD M. GILGENBACH, PROFESSOR and
Y.Y. LAU, PROFESSOR
INTENSE ENERGY BEAM INTERACTION LAB
NUCLEAR ENGINEERING AND RADIOLOGICAL SCIENCES DEPARTMENT
UNIVERSITY OF MICHIGAN
ANN ARBOR, MI 48109-2104

JULY 2002

CROSSED FIELD, HIGH ENERGY MICROWAVE SOURCE EXPERIMENTS AND THEORY
AFOSR GRANT NUMBER: F49620-99-1-0255

TABLE OF CONTENTS

1.0 EXECUTIVE SUMMARY

Relativistic magnetron experiments have successfully been accomplished utilizing the MELBA accelerator at parameters of –300 to –400 kV, 1-10 kA and pulselengths of ~0.5 microseconds. A major accomplishment has been the installation of a ceramic insulator stack, which has improved the base vacuum by a factor of 10 from 10^{-6} Torr scale to the 10^{-7} Torr scale. The Titan-Pulse Sciences magnetron is a 6-vane device operating at about 1 GHz. Microwave power has been extracted from two-opposing-cavities of this magnetron. Assuming equal output power in both arms, peak, extracted microwave power between 120 MW and 400 MW has been achieved. Microwave pulse shortening is observed with typical pulselengths in the range between 10 ns and 100 ns. Time-frequency analysis has been utilized for mode identification, indicating both the pi-mode and the 2/3 –pi mode.

The theoretical efforts were mainly concentrated in two (2) areas: (a) The first correct derivation of the limiting current in a magnetically insulated crossed-field gap in the relativistic regime, and (b) Formulation of the AC Stark broadening. Other modeling activities included collaboration with AFRL scientists concerning the coupling among cavities in the magnetron, and cathode emissions.

Close collaborations have been maintained with scientists from the Air Force Research Laboratory. AFRL simulation of the UM experiments utilizing the ICEPIC code have verified the power level as well as the delay time between the current and microwave pulse emission. The pi and 2/3 –pi mode identifications from the AFRL simulations also agree with UM experimental observations.

2.0 EXPERIMENTAL CONFIGURATION

2.1 MELBA Accelerator and Magnetron

The experimental configuration is depicted pictorially in Figure 1 and schematically in Figure 2. The magnetron, shown in Fig. 3, is a 6-vane type on loan from Titan Corporation, Pulse-Sciences Division (Dr. David Price). Microwave power is extracted by waveguide from two cavities on opposite sides. Both waveguides are terminated in UM built water loads and power is monitored by calibrated (-60 dB) coupling loops in one arm. In order to detect low frequency, competing modes that are cutoff to the waveguide, we have installed B-dot loops at the exit windows. Signals are transmitted by coaxial cable to the Faraday cage where they are diagnosed for power and time-frequency spectrum.

A major accomplishment of this research project was the installation of a ceramic insulating stack, redesigned and rebuilt by Titan, Pulse Sciences. The relativistic magnetron has been successfully operated on MELBA-C (ceramic insulator). The base vacuum has been improved by a factor of ten from 3×10^{-6} Torr to 3×10^{-7} Torr.

The MELBA cathode is extended out of the vacuum chamber and into the magnetron by a 1.27cm diameter aluminum rod that acts as the cathode stalk. Four types of cathodes were employed in these experiments, depicted in figures 4 and 5. The first cathode (A) had a rounded, aluminum, electron emission knob that ended in the center of the magnetron vanes; this cathode exhibited a high percentage of endloss current. The encapped cathodes were based on a design suggested by T. Spencer and AFRL scientists to reduce endloss current. These cathodes, extended axially beyond the magnetron vanes, but employed a strip of graphite-felt (or cotton) fibers, which acted as the electron emission region; metal balls act as the endcaps, designed to suppress breakdown. Cathodes A and B utilized Glyptal to prevent emission. Cathodes C and D used polished aluminum to permit improved vacuum with the ceramic insulator. The third and fourth (C, D) cathodes utilized double end caps outside the vanes with a cotton emitting strips of different lengths. Cathode stalk current was monitored by a B-dot loop inside the MELBA oil tank, outside the plastic insulator stack. The ceramic insulator had a large Rogowski coil installed in the accelerator flange. The endloss electron beam current was measured by an axial current collector, which transported the current through a Pearson current transformer.

Magnetic fields are generated by two electromagnets obtained on loan from Dr. Tom Spencer at the Air Force Research Lab. We modified our capacitor bank to achieve the higher (2.5-4 kGauss) magnetic fields required for these experiments. Magnet operation has been reliable to these levels.

3.0 EXPERIMENTAL RESULTS

Microwave cold tests were performed on the relativistic magnetron, as well as MAGIC code simulations, shown in Fig. 6. Results show that the pi-mode frequency has a cold-frequency of about 1.04 GHz. The 2/3 pi mode is slightly lower at 1.02 GHz. Both of these frequencies are expected to be shifted by beam loading, a phenomenon which is not understood at this time.

Relativistic magnetron experiments have been performed in the lowered range of MELBA parameters:

Voltage = ~-300 kV to -400 kV,

Diode current = 1-10 kA,

Pulselength =~0.5 microseconds.
The operating regime on a typical magnetron chart of voltage versus magnetic field is depicted in Figure 7. It can be seen that microwaves were produced near the Buneman-Hartree resonance condition, as expected, on both MELBA and its upgrade, MELBA-C.

Experimental data signals are presented in Figure 8 in a shot that was taken with the latest double-endcap cathode (D) on the upgraded MELBA-C. This shot (M10219) generated a total peak power into 2 waveguides of some 190 MW. The endloss current was roughly 20% of the total 5 kA cathode stalk current at the time of peak microwave emission with this cathode. This is much lower than the 50% endloss from the original cathode (A).

Figure 9 shows the heterodyne detector signal and time-frequency-analysis of the signal from the same shot (M10219). The TFA frequency in the lower TFA plot shows that the frequency of oscillation is 1.05 GHz during the roughly 40 ns high power pulse duration. Thus, for this shot, the oscillation appears to remain in one mode, believed to be the pi mode. Figure 10 presents a detailed time frequency analysis of shot M10202. *The remarkable aspect of this TFA analysis is that the microwave oscillation appears to persist for nearly a microsecond, albeit at a low power level for all but the 40 ns high power pulse.* The initial oscillation phase (A) has a frequency of 1.05 GHz (pi mode). During the high power phase (B), when the current has ramped to some 5-6 kA, the high power microwave pulse (~100 MW total in both waveguides) is emitted at 1.03 GHz, believed to be either the downshifted pi mode or possibly the 2/3 pi mode. After the high power pulse, in phase C, mode competition sets in, as indicated by the TFA frequency of 0.915 GHz. Finally, after MELBA is crowbarred, phase D, the magnetron continues to oscillate at low levels at 0.915 GHz. These data indicate that mode competition is a serious problem that may limit the power and pulselength of the relativistic magnetron.

In the previous report, 200 MW to 300 MW was reported with cathodes A and B, on the old MELBA (plastic insulator), twice the single-arm power shown in Figure 11; vacuums were in the range of 10^{-6} Torr. Figure 12 summarizes recent relativistic magnetron power measurements as a function of magnetic field in MELBA-C (ceramic insulator) with vacuum in the range of 10^{-7} Torr. Total extracted microwave power generation was typically in the range from 120-170 MW with cathodes C & D.

Frequency data are plotted as a function of magnetic field in Figure 13. Here, it can be seen that oscillation exists primarily in 3 modes, believed to be the Pi mode centered around at 1.03 GHz, 2/3 –pi mode at about 1.0 GHz, and an unidentified mode at 0.965 GHz.

Microwave power versus pulselength data are summarized in Figure 14. It can be seen that some of the longest pulse, high power microwave pulses were obtained with the improved vacuum on MELBA-C, with cathodes C and D.

Finally, the relativistic magnetron efficiencies are in the range from 13-18%.

4.0 THEORY

The theoretical efforts were mainly concentrated in two (2) areas: (A) The first correct derivation of the limiting current in a magnetically insulated crossed-field gap in the relativistic regime, and (B) Formulation of the AC Stark broadening. They are described below. Other modeling activities include collaboration with AFRL scientists concerning the coupling among cavities in the magnetron, and cathode emissions, but they will not be described further.

A. Limiting current in a relativistic, magnetically insulated diode

The Child-Langmuir Law is the most fundamental law for all vacuum electronic devices. It gives the maximum injected current in a nonmagnetized diode. Strictly speaking, the maximum injected current for a time-independent cycloidal flow in a relativistic, crossed-field diode has never been correctly solved, even for the one-dimensional, planar geometry. We have now provided the solution to this fundamental problem [1].

It has always been taken for granted that the maximum current that can be admitted into a gap is attained when there is sufficient space charge in the gap to force the electric field on the emitting surface equal to zero. Under this condition, additional electrons with zero emission velocity will be returned to the cathode and a virtual cathode is formed. This condition of zero surface electric field is known as the space charge limited (SCL) condition. In a nonmagnetized diode, the maximum emission current density is indeed given by the SCL condition for electrons with zero emission velocity. Surprisingly, Christenson [2] discovered that the maximum emission current density was *not* given by the SCL condition for a deeply nonrelativistic cycloidal crossed-field flow, even if the electrons are emitted with essentially zero velocity. Thus, the classic solution of Lovelace and Ott [3], who calculated the equilibrium relativistic cycloidal flows in a magnetically insulated gap under the SCL assumption, needed to be revised.

Relaxing the SCL condition, we have obtained a set of universal curves that give the maximum current density at various gap voltages [Fig. 15]. These curves reduce to the established results in the deeply nonrelativistic regime. They have been spot-checked against a 2-dimensional particle-in-cell code, which is fully relativistic and fully electromagnetic [Fig. 16]. It is interesting to note that the maximum amount of charge that can be held in a magnetically insulated diode is, in general, higher than that predicted from the SCL condition, though the physical reason remains unclear. Our work [1] was recently submitted to Phys. Rev. Lett.

B. AC Stark Broadening

During the earlier phase of this research, an attempt was made to analyze the degree of broadening of the spectra, as a result of a strong RF electric field, in the H-alpha and in the H-beta lines. The observed spectral broadening may then be used to infer the RF field in the relativistic magnetron.

AC Stark broadening has been studied in the past, but its utility is somewhat limited because it is computationally intensive, requiring many Bessel functions with large arguments and large orders. The Investigators have re-examined this problem, and have found an alternate representation of the spectral broadening, which sheds considerable insight the distribution of the broadened spectral lines. In fact, the algorithm has further been extended to include both a *combined* AC and DC electric field, which is ideally suitable for the analysis of the operating conditions in a relativistic magnetron, and possibly other HPM sources. This work has not been completed because of change of personnel midway of this research program.

5.0 References:

[1] M. Lopez, Y. Y. Lau, R. M. Gilgenbach, D. W. Jordan, and J. W. Luginsland, "Limiting current in a relativistic, magnetically insulated gap," Phys. Rev. Lett. (submitted, 2002).

[2] P. J. Christenson, PhD dissertation, University of Michigan, Ann Arbor (1996).

[3] R. V. Lovelace and E. Ott, Phys. Fluids **17**, 1263 (1974).

6.0 UM Collaborations with Air Force Research Lab Scientists

University of Michigan personnel have collaborated extensively with researchers from the Air Force Research Labs. AFRL Scientists have repeatedly visited UM, including: Tom Spencer, Mike Haworth, John Luginsland, Ryan Umstattd and Don Schiffler. UM and AFRL scientists have coauthored numerous journal papers and conference articles (see following section). AFRL scientists (Keith Cartright and Mike Haworth) successfully used ICEPIC Code to simulate the UM –Titan magnetron, leading to new insights into mode competition in the operation of this device. AFRL simulation of the UM experiments utilizing the ICEPIC code have verified the power level as well as the delay time between the current and microwave pulse emission. The pi and 2/3 –pi mode identifications from the AFRL simulations also agree with UM experimental observations. These simulations also served to benchmark the ICEPIC code. Y.Y. Lau also visited AFRL to work directly with Cartright, Umstattd and Luginsland. This collaboration led to an Invited Talk at The 2001 APS Division of Plasma Physics Meeting.

7.0 Publications and Papers Concerning This Research

1) "Cathode effects on a relativistic magnetron driven by a microsecond electron beam accelerator", M.R. Lopez, R.M. Gilgenbach, D.W. Jordan, S. Anderson, M.D. Johnston, M.W. Keyser, H. Miyake, C.W. Peters, M.C. Jones, V. B. Neculaes, Y.Y. Lau, T.A. Spencer, J.W. Luginsland· M. Haworth, R.W. Lemke, D. Price, IEEE Trans. Plasma Science, Special Issue on High Power Microwaves, June 2002

2) M. Lopez, Y. Y. Lau, R. M. Gilgenbach, D. W. Jordan, and J. W. Luginsland, "Limiting current in a relativistic, magnetically insulated gap," Phys. Rev. Lett. (submitted, 2002).

3) J.W. Luginsland, Y.Y. Lau, R.J. Umstattd, " A Review of Recent Results on Multidimensional Space Charge Limited flow", Physics of Plasmas 9, 2371 (2002) (also Invited Talk at The 2001 APS Division of Plasma Physics Meeting).

Conference Papers with Published Proceedings

1) "Relativistic L-Band Magnetron Experiments Driven by a Microsecond e-Beam Accelerator", M.R. Lopez, R.M. Gilgenbach, C. Peters, H. Miyake, S. Anderson, M. Johnston, M. Keyser, M.L. Brake, Y.Y. Lau, T.A. Spencer [a] J.W. Luginsland,[a] R.W. Lemke,[b] D. Price,[c] L. Ludeking,[d]
SPIE Conference, April 17, 2001, Orlando, FL, in press as SPIE Proceedings

2) "Application of Discrete Prolate Spherical sequences to Time-Frequency Analysis", C. Peters, Williams, Gilgenbach, Lau, et al, SPIE Conference Aug. 5, 2000, San Diego, CA, in press as SPIE Proceedings

3) "Long-Pulse Relativistic Magnetron Experiments",
M.R. Lopez, R.M. Gilgenbach, Y.Y. Lau, S. Anderson, M.D. Johnston, M. Keyser, H. Miyake, C. Peters, D. Jordan, V.B. Neculaes, T.A. Spencer J.W. Luginsland, M. Haworth, R.W. Lemke, D. Price, L. Ludeking,
SPIE Conference, April, 2002, Orlando, FL, in press as SPIE Proceedings

Conference Papers with Published Abstracts

4) " Experiments on Relativistic vs. Nonrelativistic Magnetrons, M.R. Lopez, R.M. Gilgenbach, S. Anderson, H. Miyake, C. Peters, M. Keyser, M.L. Brake, Y.Y. Lau, J.W. Luginsland, T.A. Spencer, D. Price, L. Ludeking, 42nd Annual Meeting of the APS Division of Plasma Physics, Oct. 23-27, 2000, Quebec City Canada, abstracts published in Bull. Am. Phys. Soc. vol. 45, No. 7, Oct. 2000

5) "Relativistic L-Band Magnetron and Nonrelativistic
Oven Magnetron Experiments", M. R. Lopez, R. M. Gilgenbach, S. A. Anderson, H. Miyake, C. W. Peters, M. Keyser, M. D. Johnston, M. L. Brake, Y. Y. Lau. J. W. Luginsland and T. A. Spencer, R. W. Lemke, D. Price, L. Ludeking, presented at the 2001 IEEE ICOPS PPC, Las Vegas, Nevada, June 18-22, 2001

6) Relativistic and Nonrelativistic Magnetron Experiments and Theory of Crossed Field Limiting Currents", M. R. Lopez, R.M. Gilgenbach, Y.Y. Lau, V. B. Neculaes, D.W. Jordan, M.D. Johnston, M.C. Jones, T.A. Spencer, J. W. Luginsland, M. Haworth, R.W. Lemke, David Price, presented at the 2002 IEEE ICOPS Banff, Canada, 2002

7) "Experiments on relativistic 100's MW magnetrons and low voltage, kW magnetrons", Lopez, Gilgenbach, Lau, V. B. Neculaes, D.W. Jordan, M.D. Johnston, M.C. Jones, T.A. Spencer, J. W. Luginsland, M. Haworth, R.W. Lemke, David Price, 43rd Annual Meeting of the APS Division of Plasma Physics, Long Beach, CA Oct. 29-Nov. 2, 2001 abstracts published in Bull. Am. Phys. Soc. vol. 46, Oct. 2001

8.0 GRADUATE AND UNDERGRADUATE STUDENT INVOLVEMENT IN PROJECT

The following, US Citizen students have been employed in this research project:

1) Mike Lopez, Ph.D. Pre-candidate

2) Scott Anderson, Ph.D. Graduate

3) Chris Peters, Ph.D. Graduate

4) Antwan Edson, Undergraduate Lab Assistant (graduated)

5) Marc Keyser, MS Graduate

6) Mark Johnston, MS Graduate

7) Michael Jones, MS candidate

8) David Jordan, MS Candidate

L-Band Magnetron on MELBA

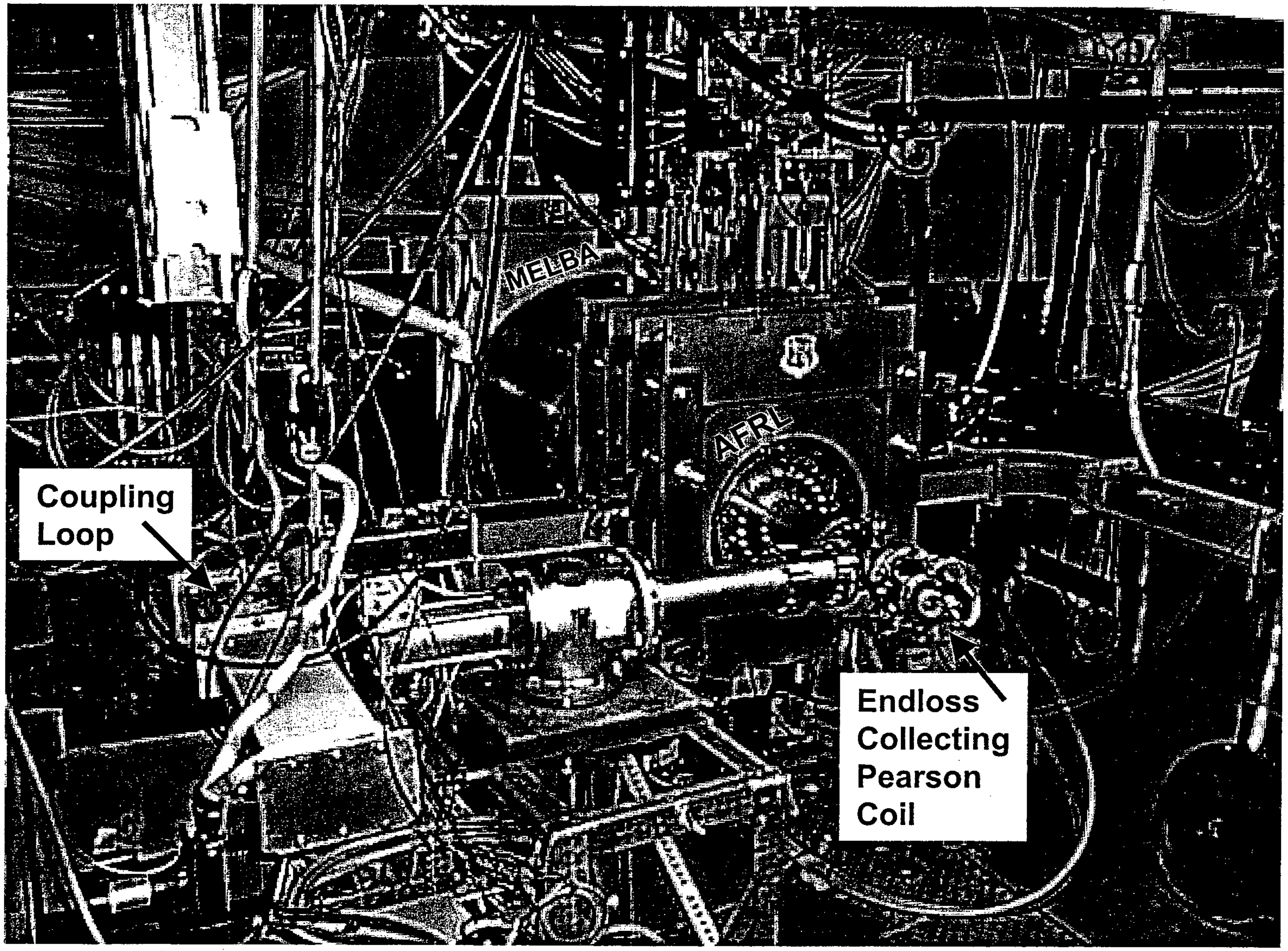

Figure 1

L-Band Magnetron from Titan Corp. on MELBA-C

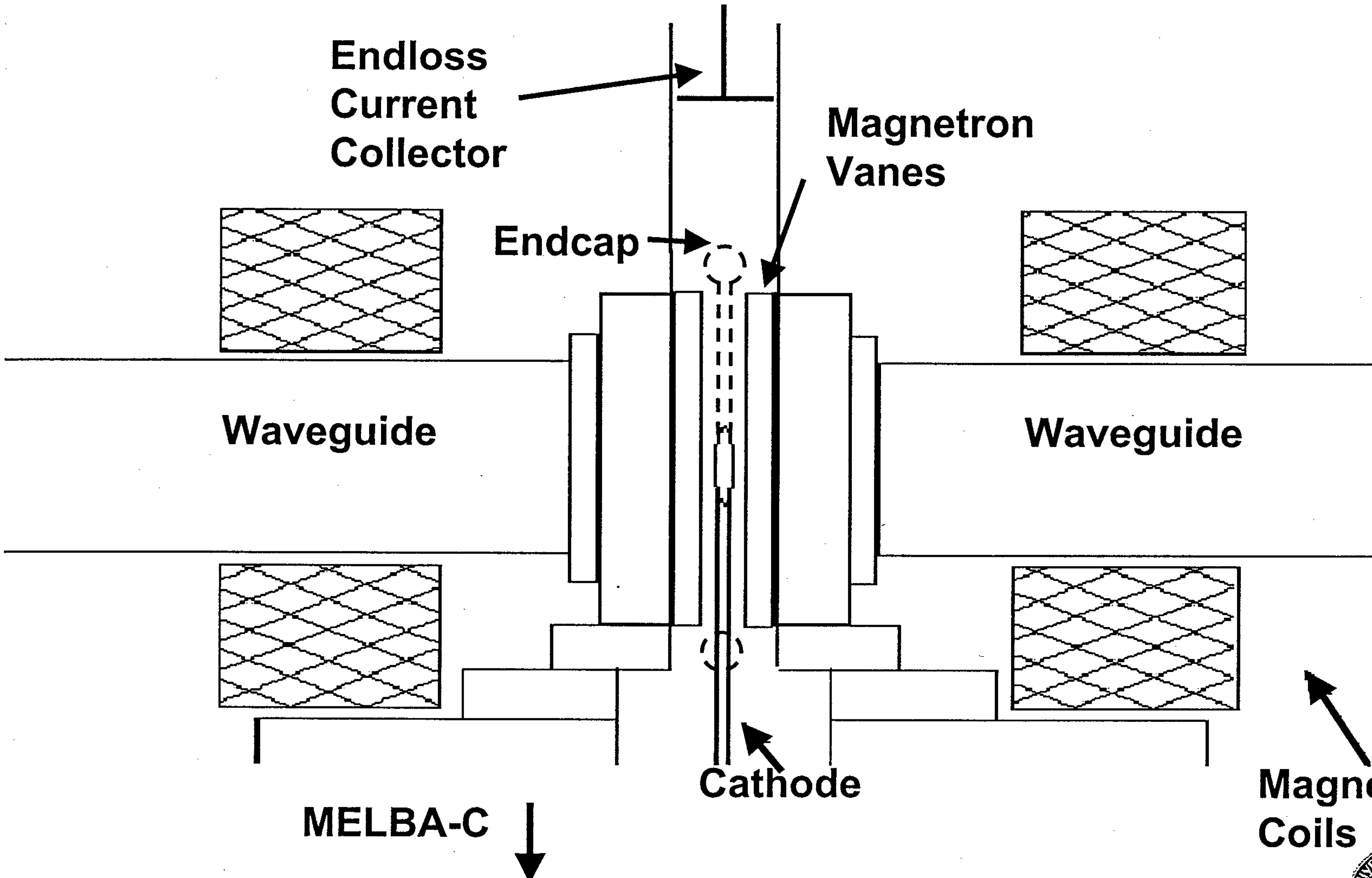

Figure 2

The L-Band Magnetron from Titan Corporation

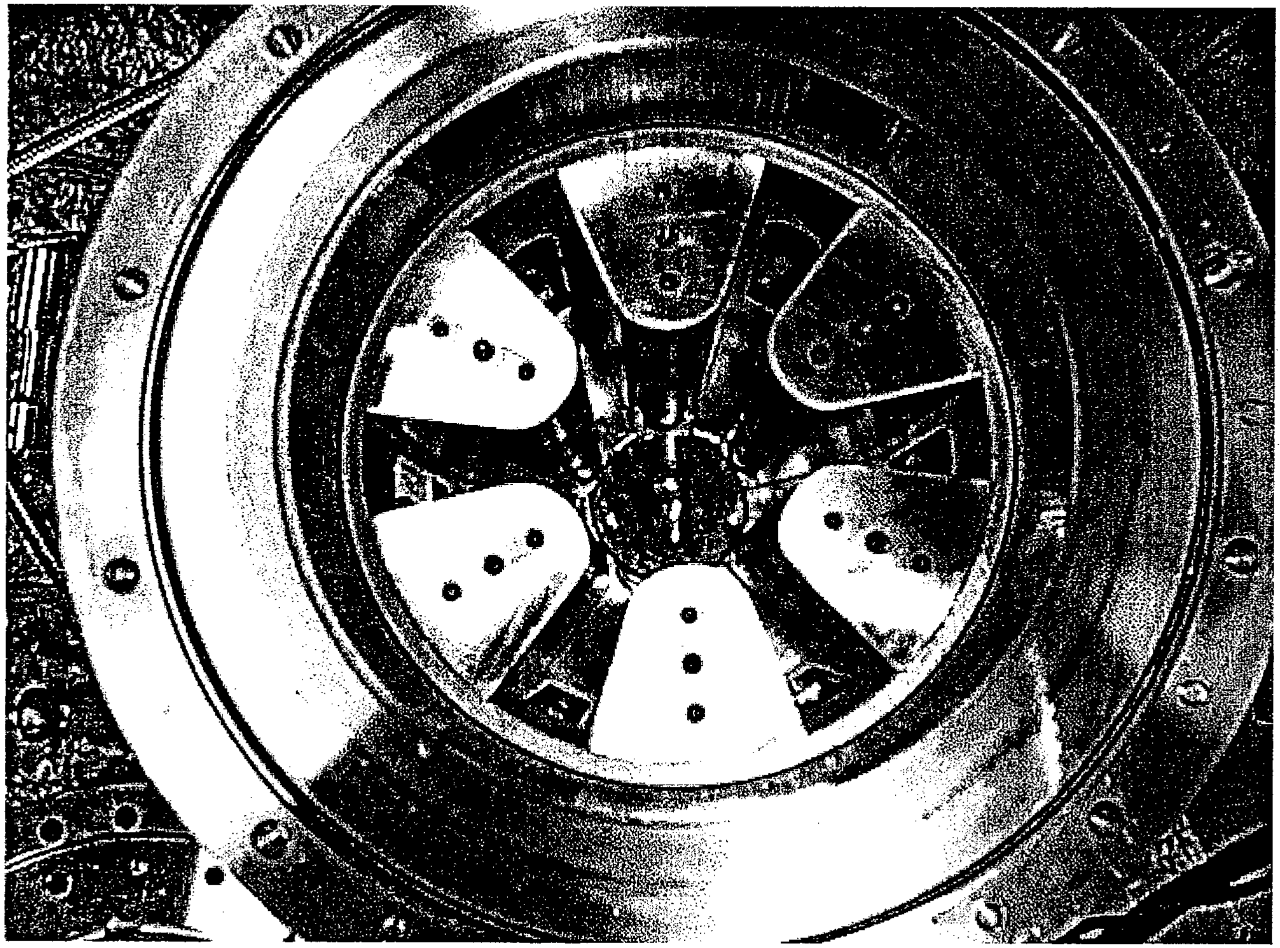

~ 17 cm

Figure 3

Cathode Designs on MELBA

(A) No-endcap Cathode

Diam. = 1.91 cm

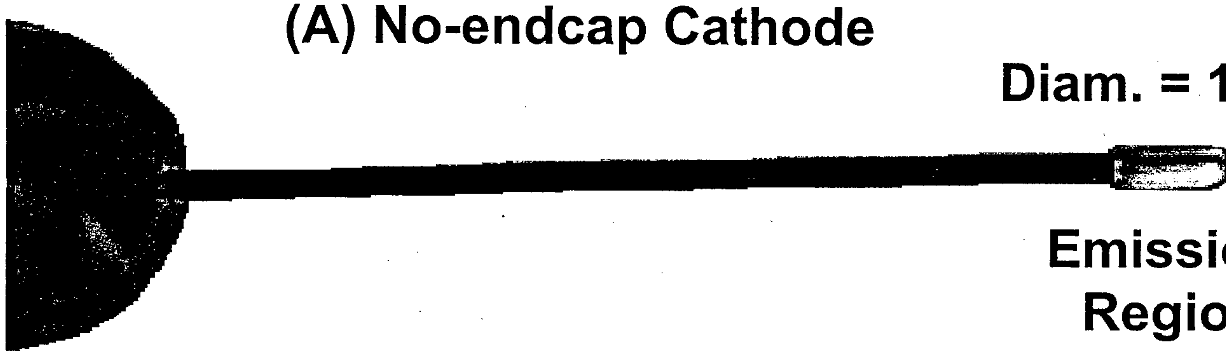

Emission Region

(B) Endcap Cathode

Diam. = 1.27 cm

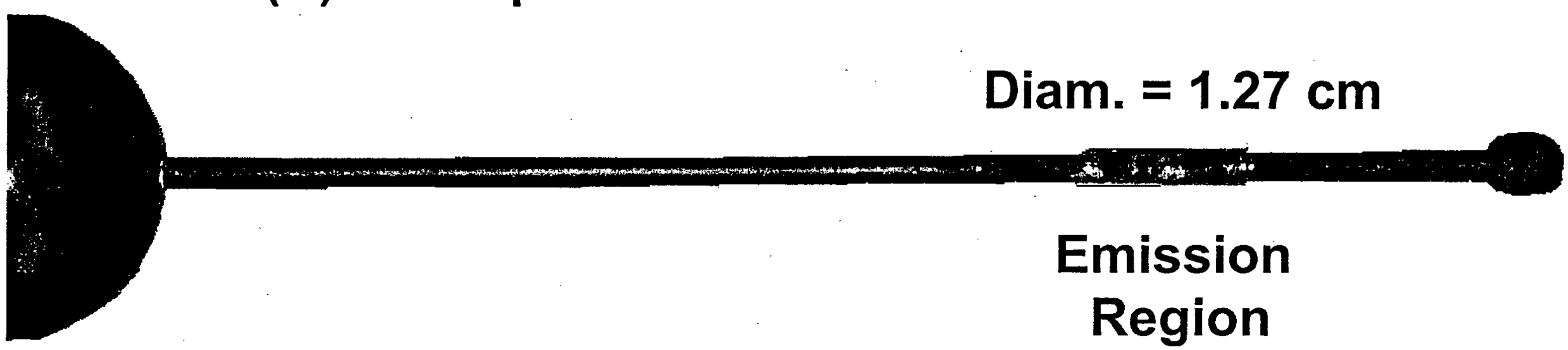

Emission Region

~ 60 cm

Figure 4

Cathode Designs on MELBA-C

(C) Dual-endcap Cathode w/ 6.5 cm felt.

(D) Dual-endcap Cathode w/ 1 cm felt.

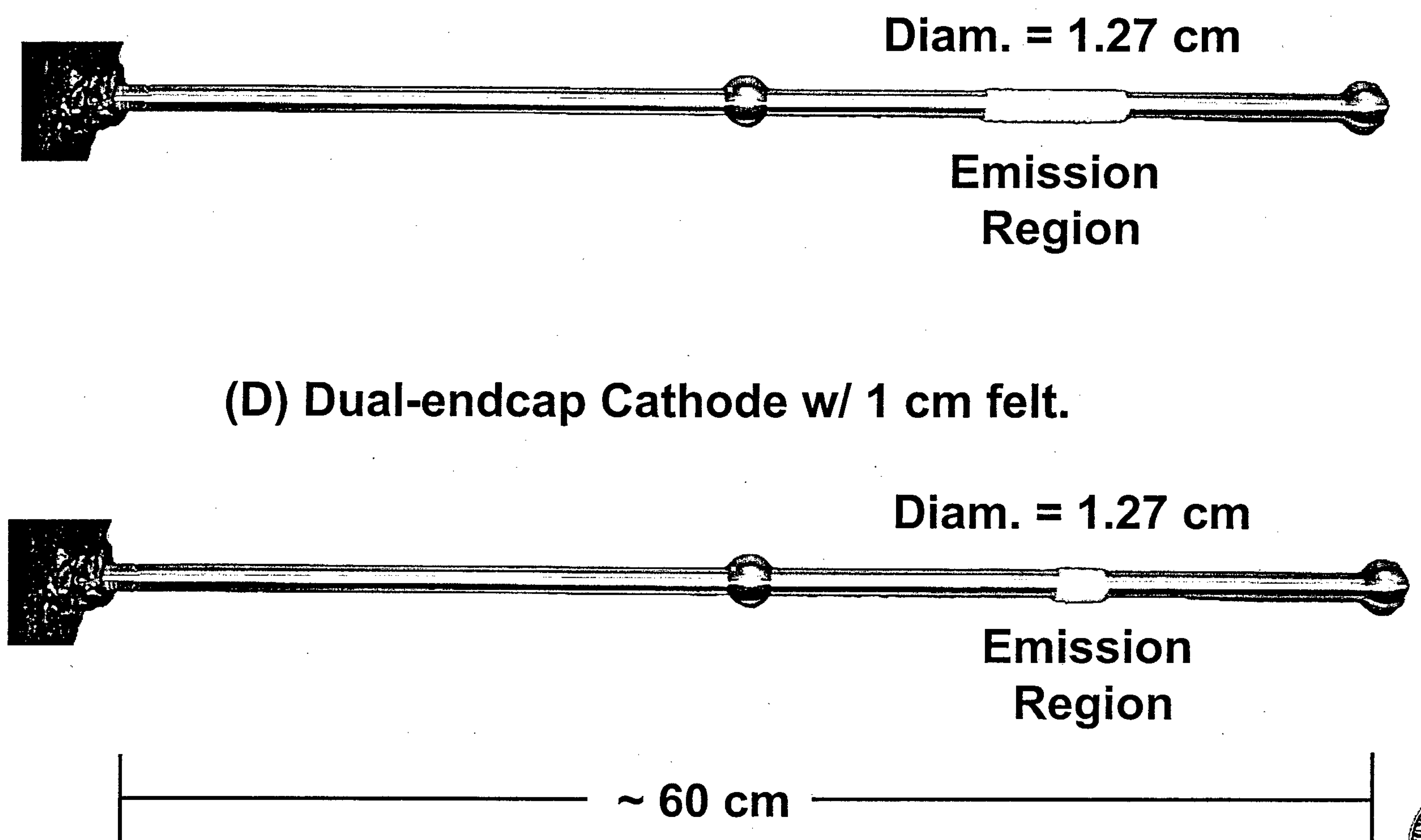

Figure 5

MAGIC & Cold Test Results

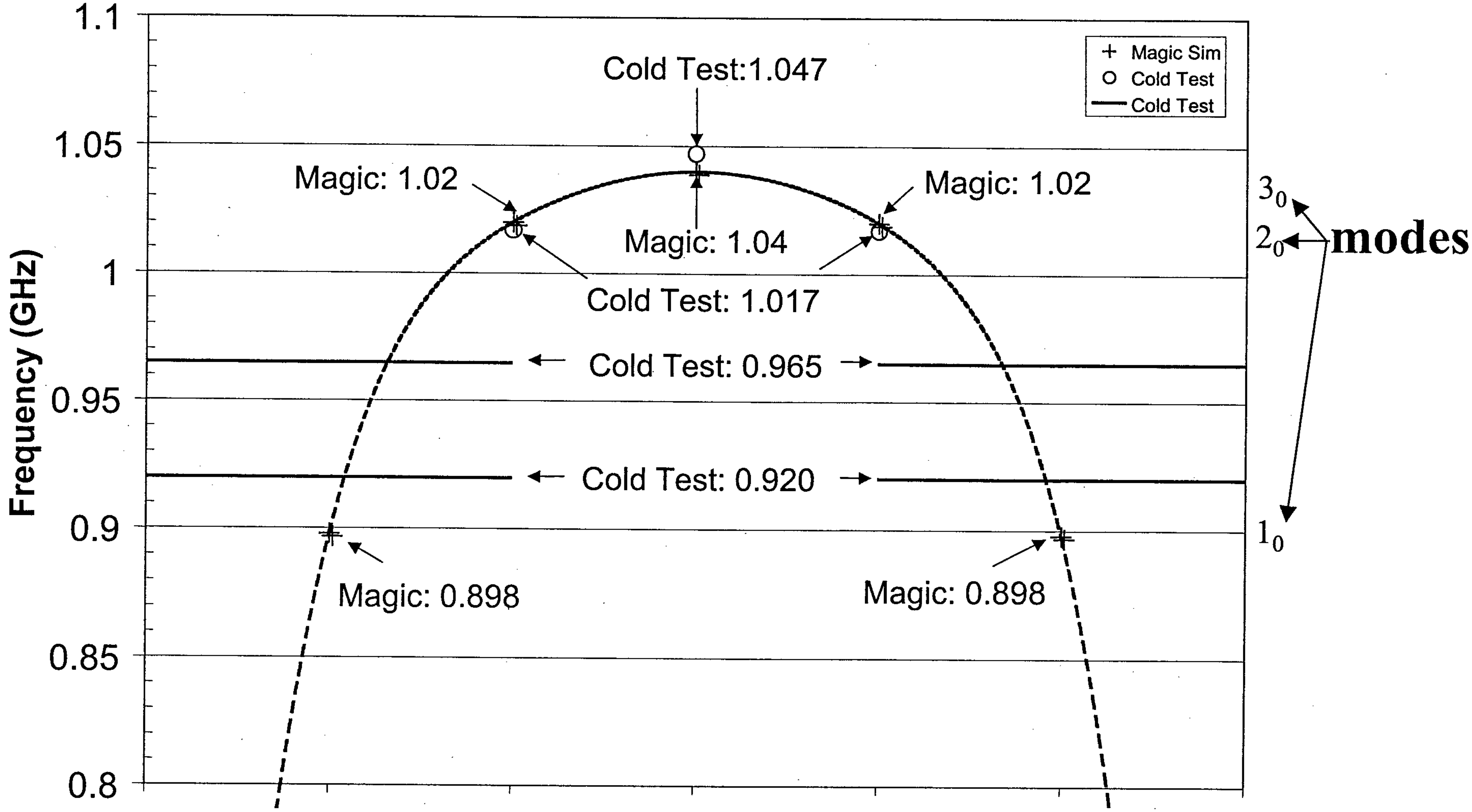

Figure 6

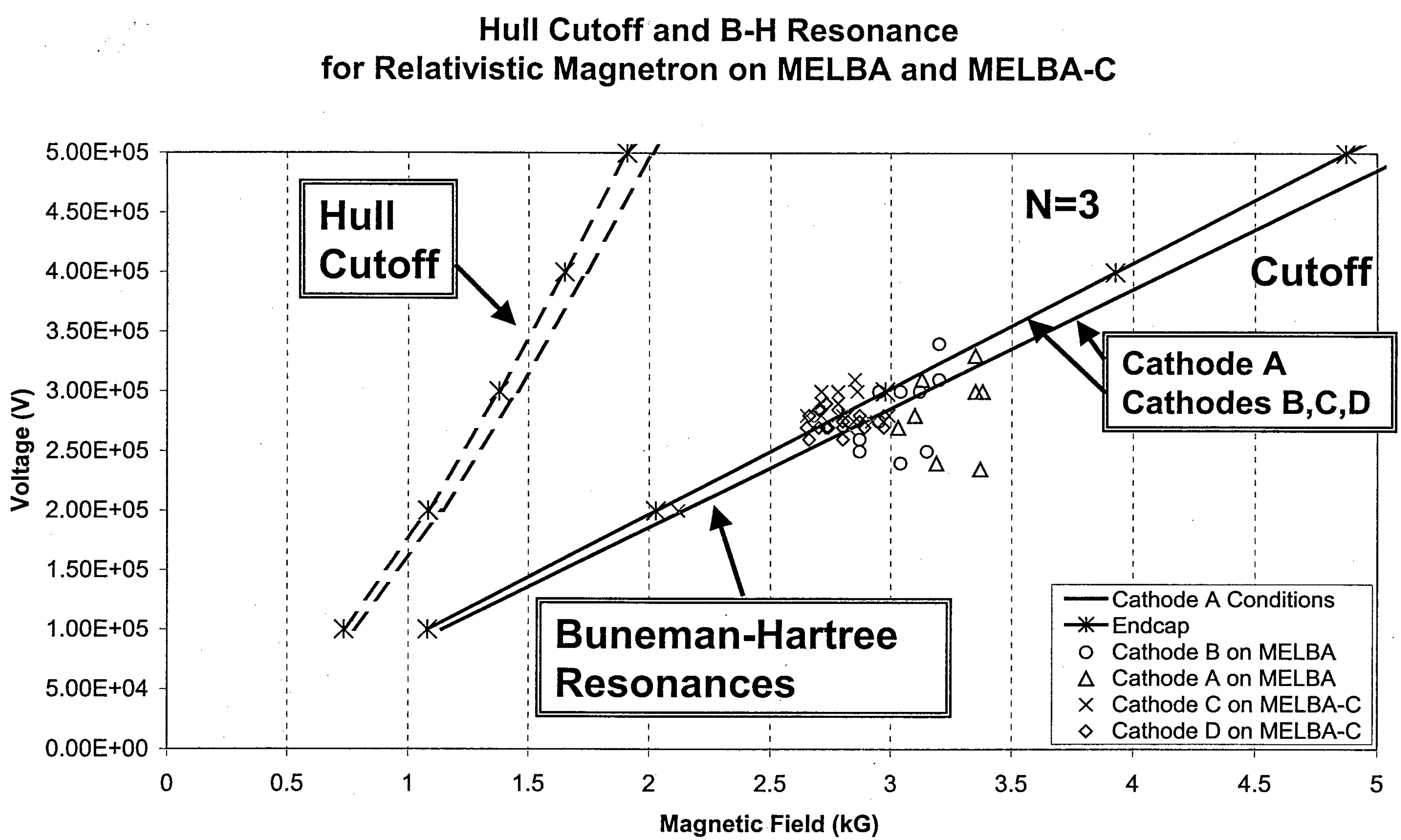

Hull Cutoff and B-H Resonance
for Relativistic Magnetron on MELBA and MELBA-C
Voltage (V)
5.00E+05
4.50E+05
4.00E+05
3.50E+05
3.00E+05
2.50E+05
2.00E+05
1.50E+05
1.00E+05
5.00E+04
0.00E+00
0
0.5
1
1.5
2
2.5
3
3.5
4
4.5
5
Magnetic Field (kG)
Hull Cutoff
N=3
Cutoff
Cathode A
Cathodes B,C,D
Buneman-Hartree Resonances
Cathode A Conditions
Endcap
Cathode B on MELBA
Cathode A on MELBA
Cathode C on MELBA-C
Cathode D on MELBA-C

Figure 7

Experimental Currents, Power, and Voltage Double-Endcap Cathode (D) on MELBA-C

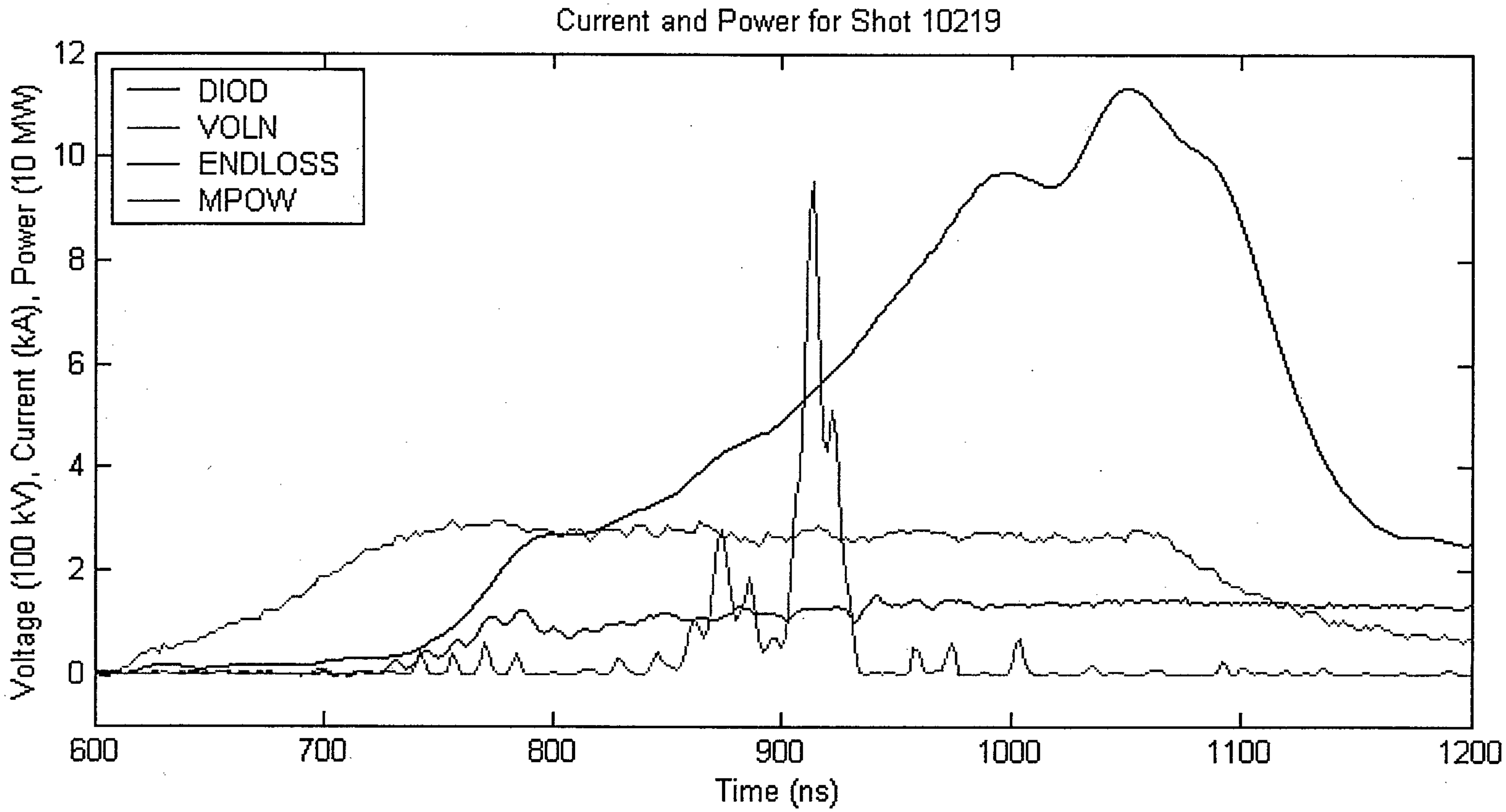

- High Power: 95 MW measured from one cavity
  190 MW total extracted
- 100 ns pulselength

Figure 8

Time-Frequency Analysis
Double-Endcap Cathode (D) on MELBA-C

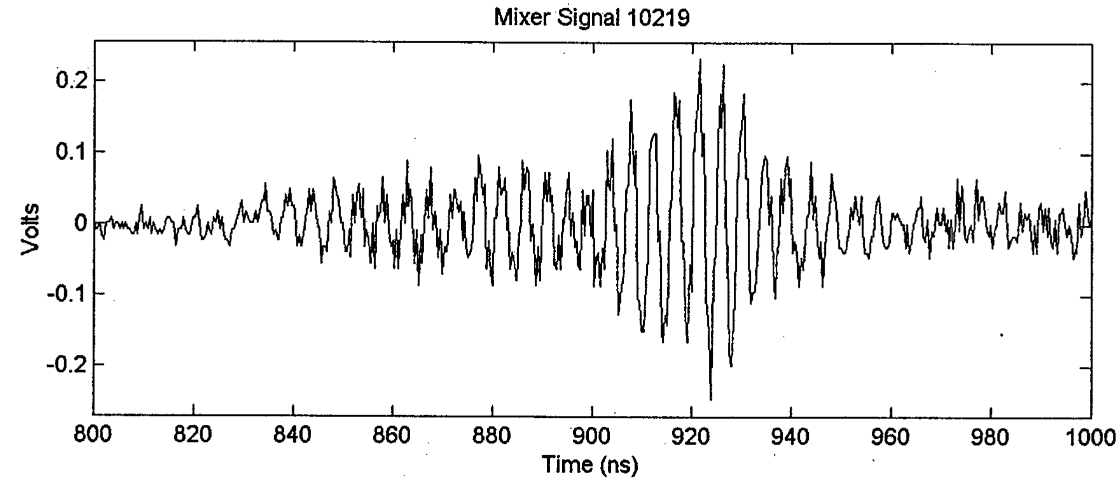

~100 ns pulse

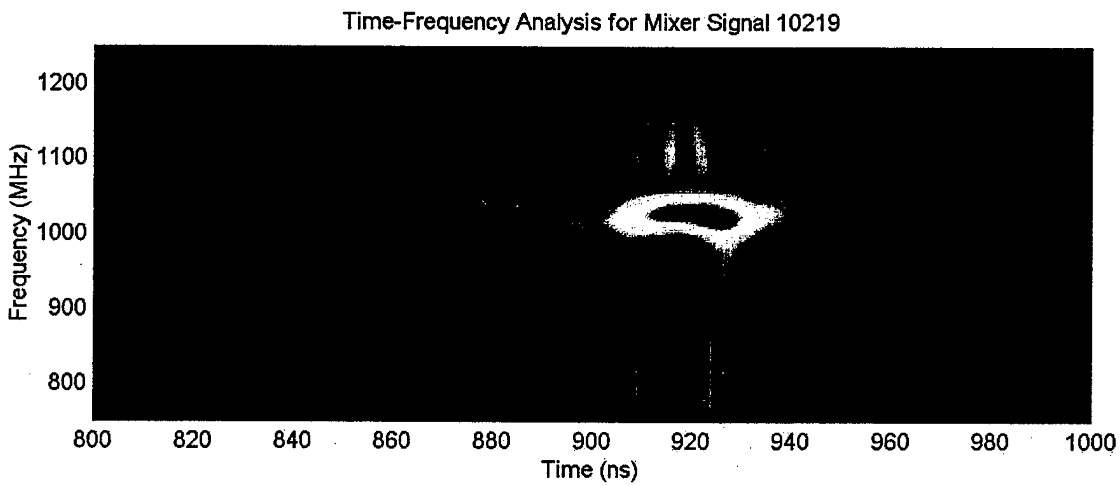

π-mode oscillation at 1.05 GHz.

Figure 9

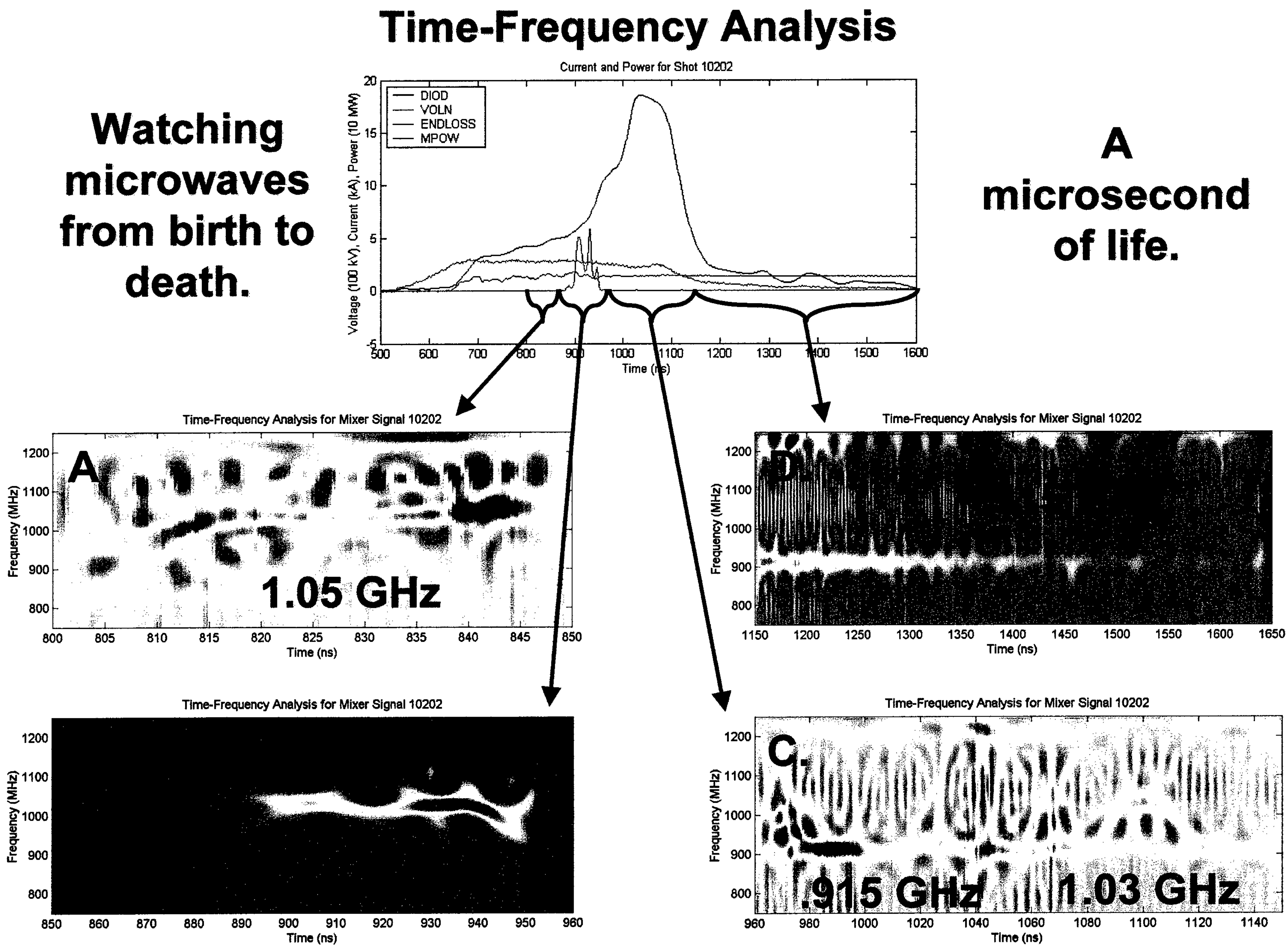
Time-Frequency Analysis
Watching microwaves from birth to death.
A microsecond of life.
Current and Power for Shot 10202
DIOD
VOLN
ENDLOSS
MPOW
Voltage (100 kV), Current (kA), Power (10 MW)
Time (ns)
Time-Frequency Analysis for Mixer Signal 10202
A
1.05 GHz
Frequency (MHz)
Time (ns)
Time-Frequency Analysis for Mixer Signal 10202
D.
Frequency (MHz)
Time (ns)
Time-Frequency Analysis for Mixer Signal 10202
Frequency (MHz)
Time (ns)
Time-Frequency Analysis for Mixer Signal 10202
C.
.915 GHz
1.03 GHz
Frequency (MHz)
Time (ns)

Figure 10

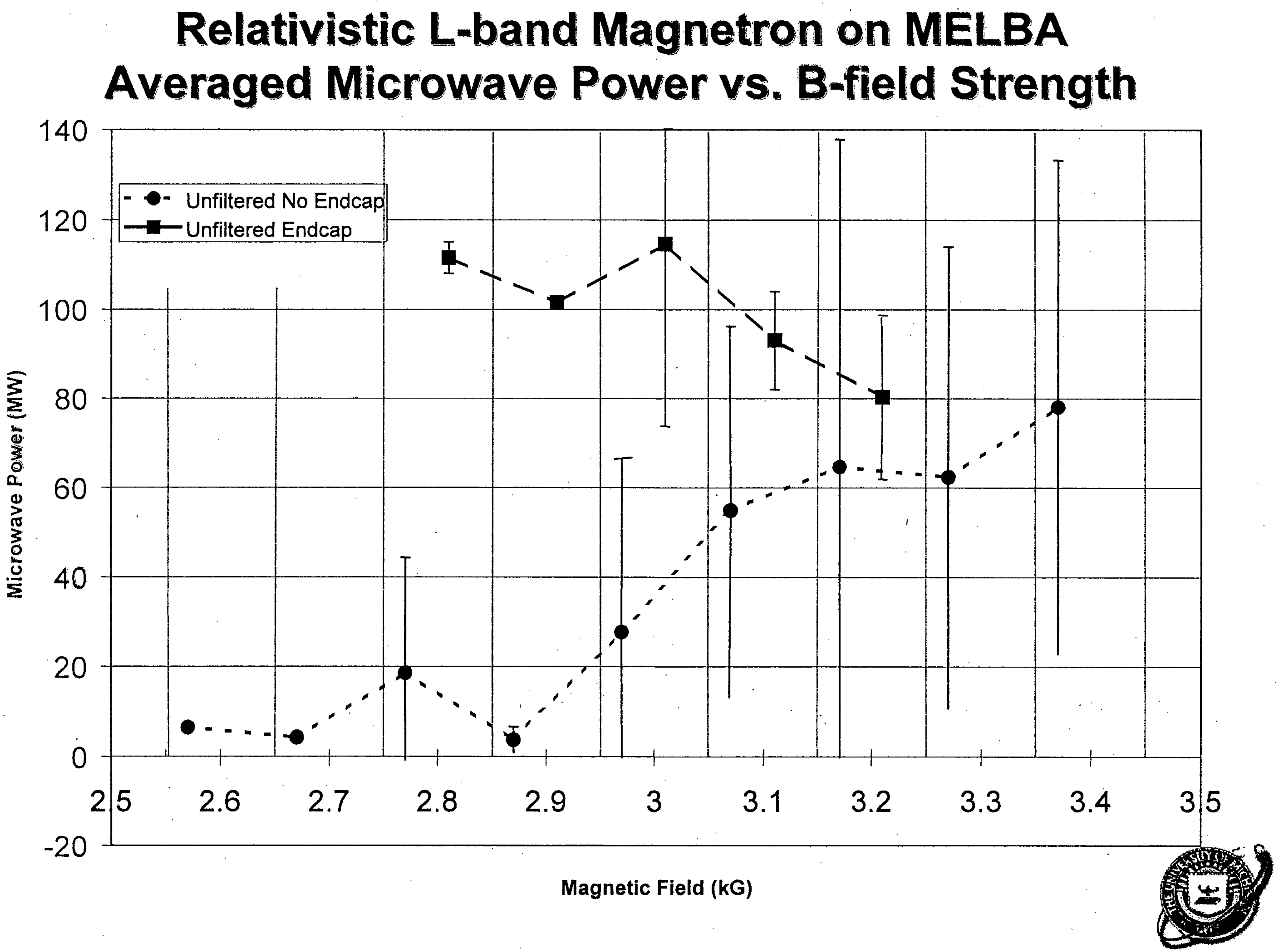

Relativistic L-band Magnetron on MELBA
Averaged Microwave Power vs. B-field Strength
Microwave Power (MW)
140
120
100
80
60
40
20
0
-20
2.5
2.6
2.7
2.8
2.9
3
3.1
3.2
3.3
3.4
3.5
Magnetic Field (kG)
Unfiltered No Endcap
Unfiltered Endcap

Figure 11

Relativistic L-band Magnetron on MELBA-C
Averaged Extracted Microwave Power vs. B-field Strength

(Actual Power = Extracted x 2)

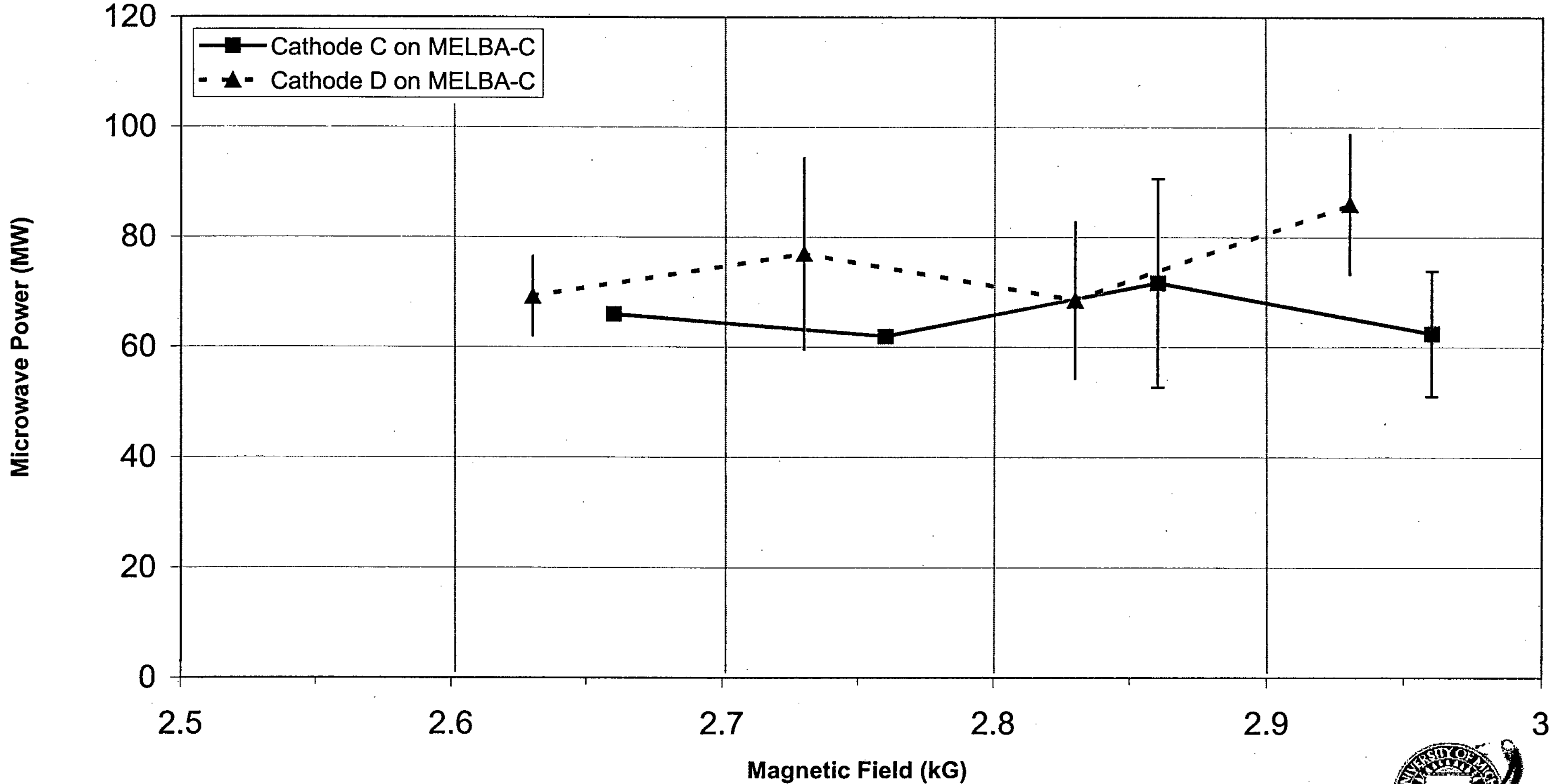

Figure 12

Relativistic L-band Magnetron on MELBA and MELBA-C Microwave Frequency vs. Magnetic Field Strength

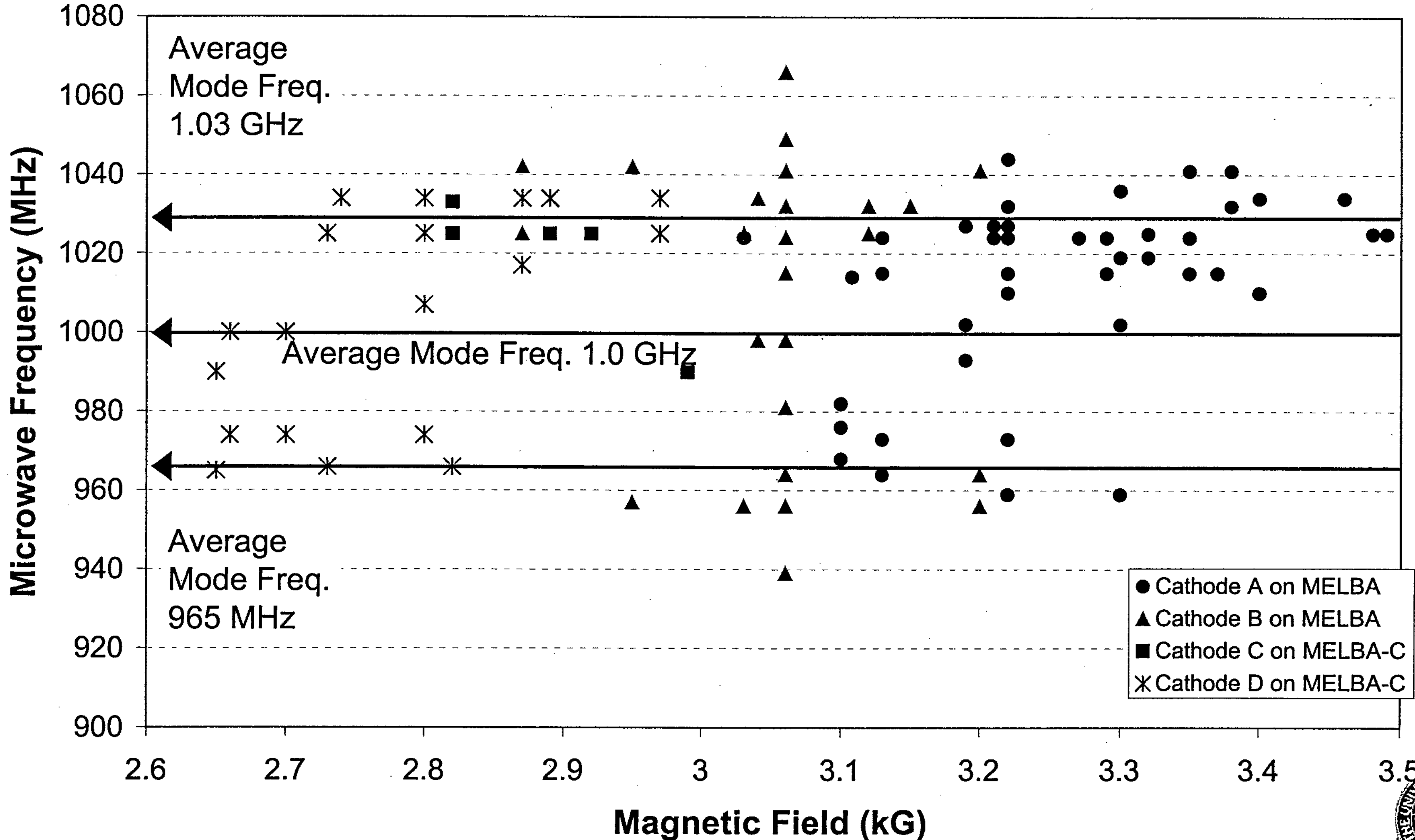

Figure 13

Microwave Power vs. Pulselength
No-encap (A) and encapped (B, C, D) cathodes

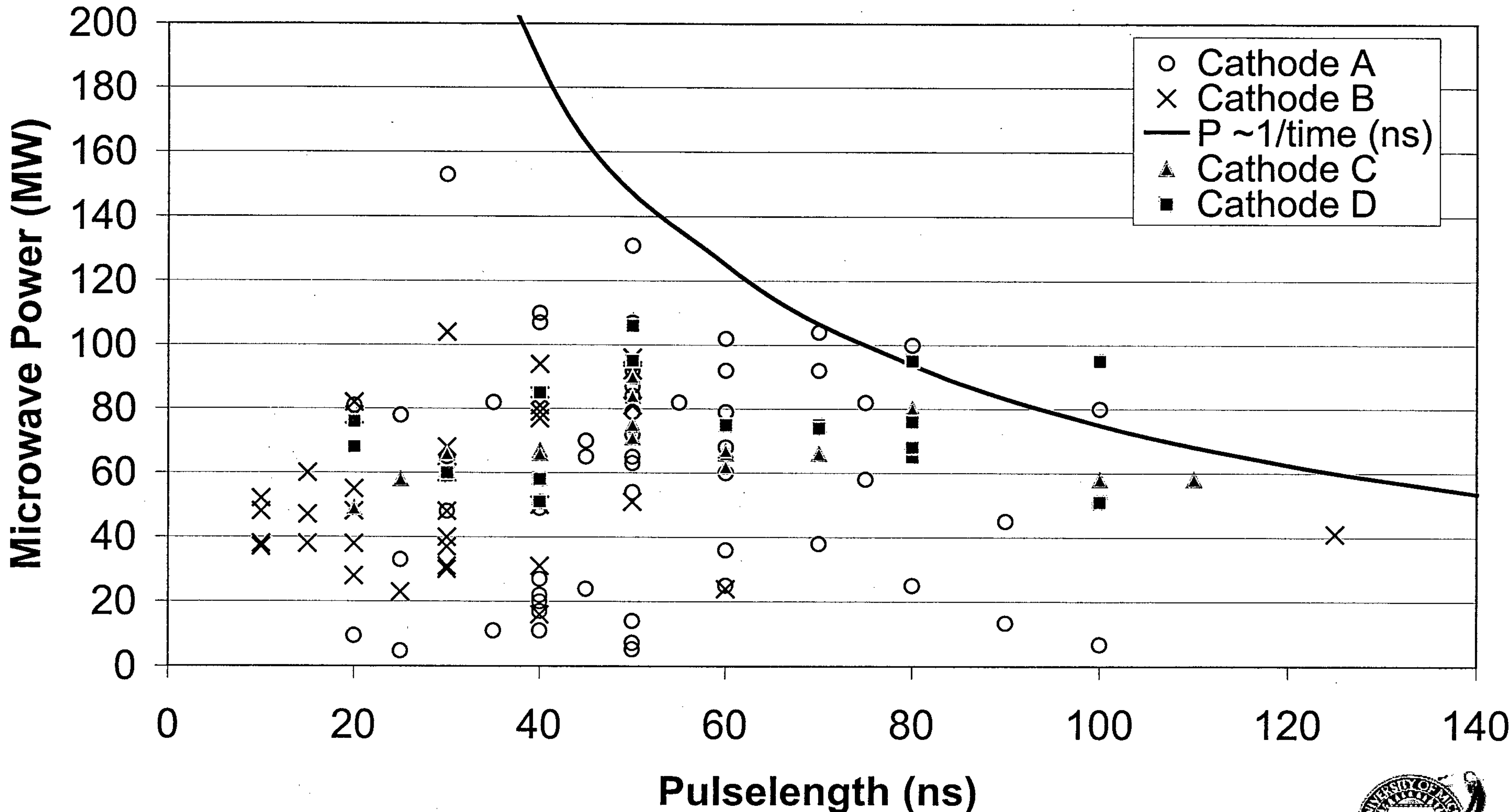

Figure 14

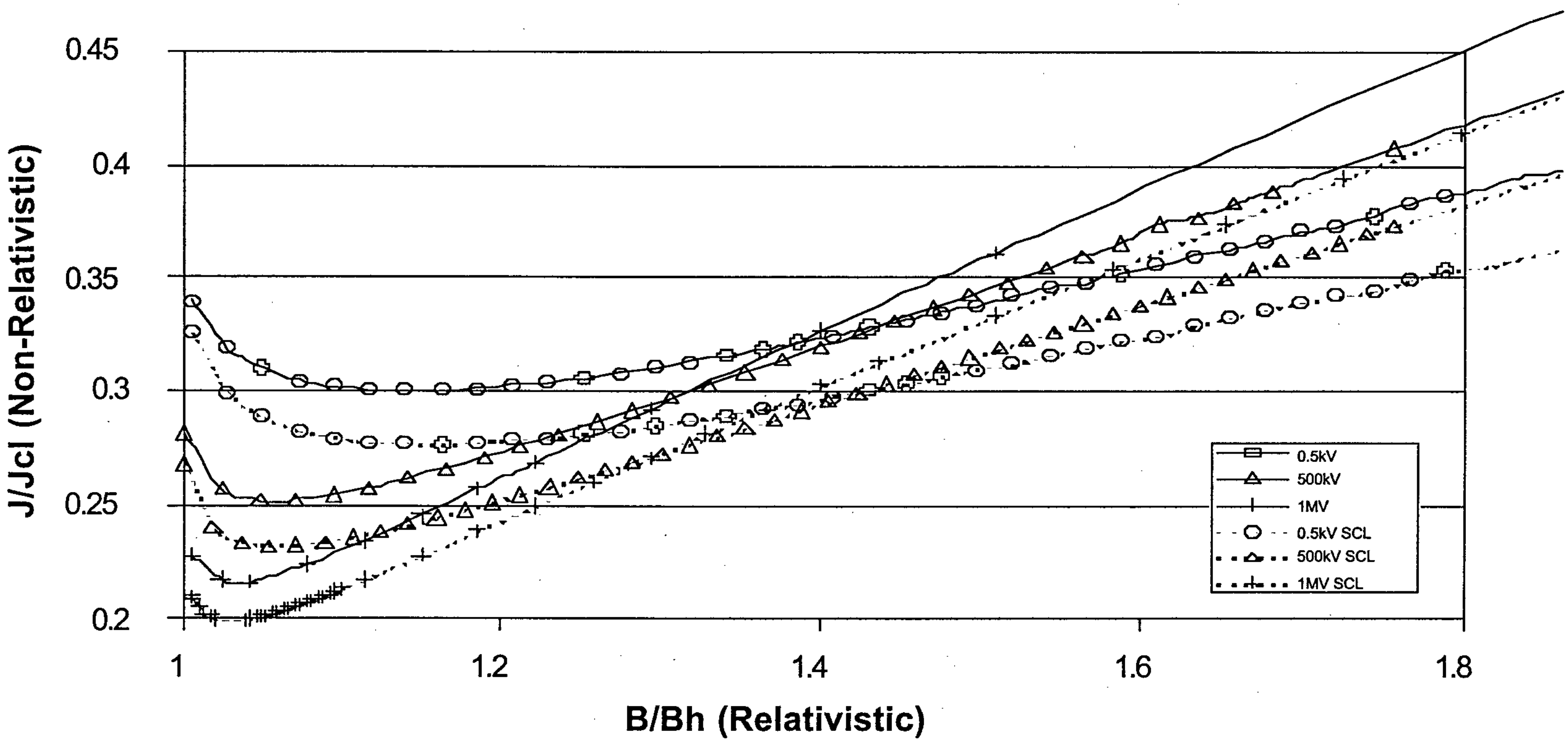

Fig. 15. The normalized limiting current density in a crossed-field gap under the condition of magnetic insulation, at various gap voltage, V. Also shown are the corresponding values when the space charge limited (SCL) condition is imposed on the cathode.

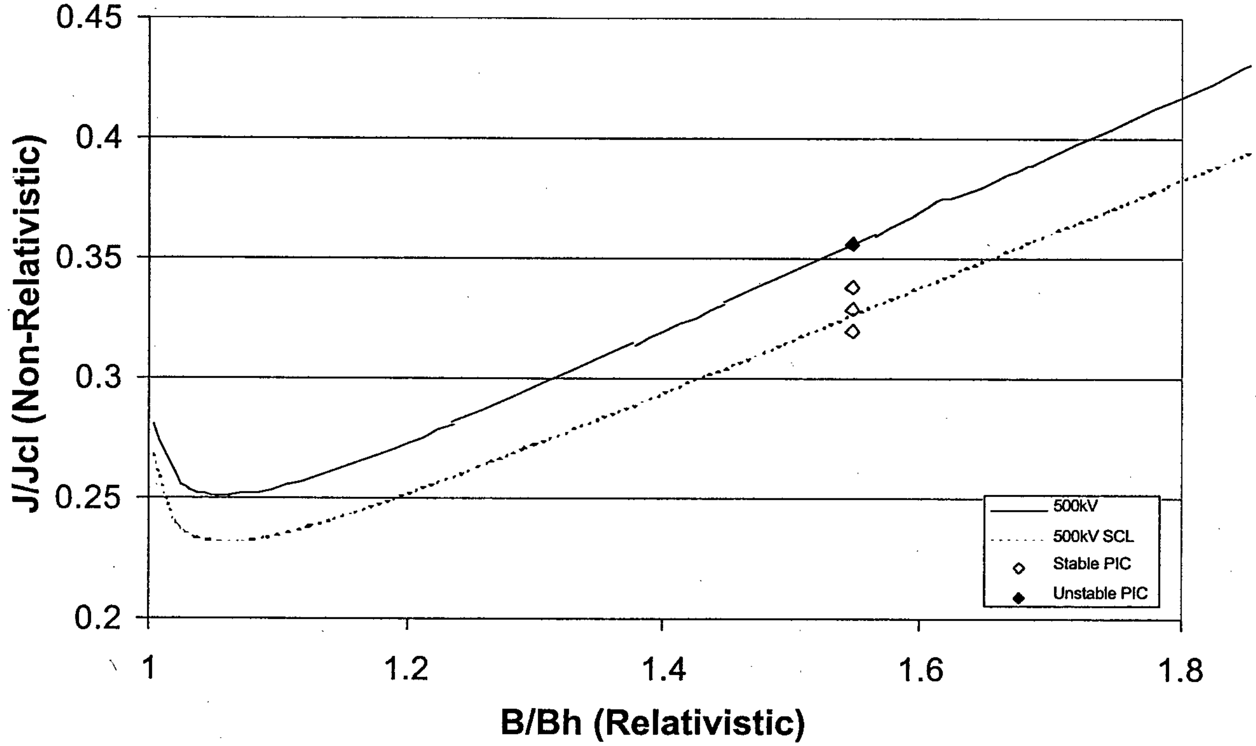

Fig. 16. MAGIC simulation data for a 500 kV diode. The two curves are reproduced from Fig. 15, with the upper curve representing the maximum injection current, and the lower curve assuming space charge limited condition on the cathode. Virtual cathode is observed in the MAGIC simulation only when the injected current reaches the upper curve.